Optics Communications 344 (2015) 21–26

Contents lists available at ScienceDirect

Optics Communications

journal homepage: www.elsevier.com/locate/optcom

# The diagnostic study of optical tomography for high-temperature flow fields in the open system

Yun-yun Chen [a,*], Xiao-gu Huang [a], Yan Wen [a], Zhen-yan Guo [b], Yang Song [b]

[a] School of Physics and Optoelectronic Engineering, Nanjing University of Information Science and Technology, Nanjing, 210044, China
[b] Department of Information Physics and Engineering, Nanjing University of Science and Technology, Nanjing 210094, China

ARTICLE INFO

*Article history:*
Received 19 November 2014
Received in revised form
9 January 2015
Accepted 12 January 2015
Available online 13 January 2015

*Keywords:*
Optical tomography
Moiré and emission tomography
High-temperature and illuminant flow field
Temperature reconstruction
Open system

ABSTRACT

In this paper, the application of moiré and emission tomography in diagnosing the high-temperature and illuminant flow field in the open system is studied, and two flames with different spatial size are chosen as typical objects. First of all, the moiré fringes and the corresponding measured two flames are obtained by integrating moiré and emission tomography. After that, the distribution and the brightness of the moiré fringes are compared for the two flame flow fields, as well as the distributions of the refractive index and the components. Then, the temperature distributions of the two flames are compared and analyzed. The results show that, when moiré and emission tomography are applied in diagnosing the high-temperature and illuminant flow field in the open system, the size, the structure and the species components of the measured flow fields have important effect on the final temperature results. Consequently, the specific problem should be specifically analyzed for the optical diagnosis of flow fields.



## 1. Introduction

Optical computerized tomography (OCT), as a branch of computerized tomography (CT), is a non-contact measurement technique and shows superiorities in many domains, such as the flow visualization and the measurement of the thermo physical parameters. Up to now, this technique has been mainly used in the structural visualization for low temperature [1,2], low and high speed complex flow fields [3–5], the density measurement [6], as well as the temperature measurement for the flow fields whose temperature is not too high [7]. Until now, it is rarely reported that this technology could be used in the structural visualization, or the temperature and the electron number density measurement for the high-temperature complex flow fields [8]. Due to the fact that molecules or atoms of a gas dissociate even ionized as the temperature increases, it becomes a kind of gas with obvious plasma characteristics. In this case, many relatively matured experimental testing methods, as well as the theory and the reconstruction model of OCT can not be directly transplanted into the diagnosis of high-temperature flow fields. In addition, it can not well visualize the real structure, because the principle of OCT is to record the refractive index variation of the measured flow fields. The current researches are restricted as the following reasons: 1) the structural visualization and diagnosis of high-temperature complex flow fields have not been well solved; 2) each method has its advantages and disadvantages in practical application for the structural visualization and parameter diagnosis of high-temperature complex flow fields; 3) A common method can not well realize the 3-D structural visualization and the accurate measurement of key parameters.

In the sight of the characteristics of different methods can solve different problem, there is no doubt that the combination of different methods is a good solution to solve the high-temperature complex flow field's structural visualization and the key parameter's measurement. Considering the following points: 1) OCT has been widely applied in the 3-D visualization and the parameters diagnosis for many flow fields [9], which means it has unique advantages in visualizing and diagnosing high-temperature complex flow fields. 2) For the illuminant flow fields, emission tomography can obtain the structure of them without an external light source, and the experimental set up is simple and easy to be realized [10]. Consequently, in this study, OCT and emission computerized tomography (ECT) are jointed to achieve the structural visualization and the key parameter's measurement for high-temperature and illuminant flow fields.

In this study, two flames with different sizes are chosen for experiment. It is hoped that the research can provide important reference for the 3-D structural visualization and the key parameter determination for high-temperature and illuminant complex flow fields. The relevant results can be further promoted and applied to various high-temperature and illuminant complex flow fields, such as the internal combustion engine, the diesel engine,

* Corresponding author.
*E-mail address:* yunqq321@sina.cn (Y.-y. Chen).

http://dx.doi.org/10.1016/j.optcom.2015.01.039
0030-4018/

the welding and the plasma cutting.

## 2. Basic theory

The refractive index of a gas flow field which is composed by a sort of neutral particles can be described by [11]:

$$n-1=\frac{1}{L}\left(A+\frac{B}{\lambda^2}\right)N_n \tag{1}$$

where $L$ is the Loschmidt number ($2.687\times10^{-19}\mathrm{cm}^{-3}$), $A$ and $B$ are the constants relevant to the specific composition [12], $\lambda$ represents the probe wavelength, and $N_n$ is the number density of neutral particles.

For a multi-composition flow field, the refractive index should meet the principle of superposition, like:

$$n-1=\frac{1}{L}\sum_i\left(A_i+\frac{B_i}{\lambda^2}\right)N_n=\frac{1}{L}\sum_i\left(A_i+\frac{B_i}{\lambda^2}\right)\gamma_i N_t$$
$$=\frac{1}{L}\left(\sum_i A_i\gamma_i+\frac{\sum_i B_i\gamma_i}{\lambda^2}\right)N_t=\frac{1}{L}\left(A+\frac{B}{\lambda^2}\right)N_t, \tag{2}$$

where $A=\sum_i\gamma_i A_i$ and $B=\sum_i\gamma_i B_i$, $\gamma_i$ represents the mole fraction of the $i$-th composition, $A_i$ and $B_i$ are the constants of the $i$-th composition, and $N_t$ denotes the total particle number density of the flow field.

According to the pressure equation in thermodynamics, we can have:

$$N_t=\frac{P}{\kappa T}, \tag{3}$$

where $\kappa$ is the Boltzmann constant, $P$ and $T$ indicate the pressure and the temperature of the flow field, respectively.

Consequently, the dependence of a flame flow field's refractive index on the temperature, the pressure and the composition could be finally written as:

$$n-1=\frac{1}{L}\left(A+\frac{B}{\lambda^2}\right)\frac{P}{\kappa T}. \tag{4}$$

According to Eq. (4), it is known that the determination of the component and the pressure for the measured flow field becomes the key step of temperature reconstruction, when the methods are based on the measurement of the refractive index. It even can be proposed that they directly determine the accusation of the parameter reconstruction, which implies the importance of the structural visualization for high-temperature and illuminant complex flow fields. This point can be attributed to the determination of species components should be on the basis of structural visualization.

## 3. Experiment and results

### 3.1. Experimental set-up

Fig. 1 simply describes the schematic diagram of experimental set up. A laser with the central wavelength 532 nm and the maximal output power of 400 mW serves as the light source. The collimating lens owns a focal length of 300 mm and a diameter of 50 mm. The imaging lenses, their focal length and diameter are 300 mm and 75 mm, respectively. Two Ronchi gratings, with a grating constant $d$ of 0.02 mm, are oriented at small angles of $+\theta/2$ and $-\theta/2$ relative to $y$-axis. For the sake of ensuring they can capture synchronously, the two CCDs are controlled by inner trigger. The experiment is achieved with the room temperature of 297 K, and the percentage purity of the propane is more than 95%.

### 3.2. Experimental results

The two measured propane-air flames obtained in experiment are shown in Fig. 2. Moreover, the deflected moiré fringes are supplied in Fig.3.

## 4. Analysis and discussion

### 4.1. Comparative study of the two flames

#### 4.1.1. Comparison of the moiré fringe distribution

From the perspective of the size of fringes region, as used in the experiment of the collimating lens is 5 cm in diameter, according to the proportion that the size of the bending area in the moiré fringe, we can roughly obtain the size of the measured flow field. By comparing Fig. 3(a) and (b), it is easy to find that there exists obvious difference in the deflective structure of the moiré fringe of the two flame flow fields, which implies that they have some difference in structure.

#### 4.1.2. Comparison of the brightness and refractive index distribution

Because the flame 1 is larger and flame 2 is smaller in the experiment, we selected the cross sections 10 mm, 20 mm of the flame 1 and 2.2 mm, 3.2 mm of the flame 2 above the jet nozzle as the examples for the comparative study. At the same time, we compared their distributions of the brightness and the corresponding refractive index. For the sake of facilitate comparing, a radial direction is chosen for the following discussion. The flames are divided into different regions on the basis of the light

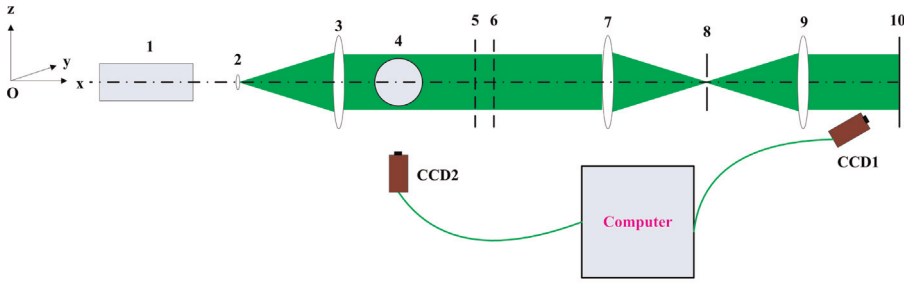


1-Laser (532nm), 2-Extender lens, 3-Collimating lens, 4-flame, 5,6-Ronchi gratings, 7,9-Imaging lens, 8-Filter, 10-Screen

**Fig. 1.** The schematic diagram of experimental set up.

Please cite this article as: Y.-y. Chen, et al., Optics Communications (2015), http://dx.doi.org/10.1016/j.optcom.2015.01.039